Geophysical Journal International

Geophys. J. Int. (2022) **231,** 1535–1544
Advance Access publication 2022 July 11
GJI Seismology

https://doi.org/10.1093/gji/ggac265

Day–night cycle of seismic noise HVSR and comparison with body waves and *T* waves

Mario La Rocca and Giuseppe Davide Chiappetta

Università della Calabria, Via P. Bucci 12*B*, 87036 *Rende (CS), Italy. E-mail: mario.larocca@unical.it*

Accepted 2022 July 8. Received 2022 June 24; in original form 2021 December 31

SUMMARY

We analysed long (months) continuous recordings of ground motion at more than 30 sites in Calabria (Italy) in order to investigate the relationships among background signal amplitude, noise composition, day–night cycle and horizontal to vertical spectral ratio (HVSR). We computed the root mean square (rms), polarization and HVSR of the seismic signal. For many sites, the HVSR contains at least one well-defined peak of amplitude greater than 2 that is representative of site effects produced by the shallow geological structure and/or topography. At six of the investigated sites, we observe an important variation of the HVSR peak amplitude that is well correlated with the day–night cycle, the peak amplitude being greater during day hours, when the background signal amplitude is higher. The rectilinearity of particle motion computed from the polarization analysis is higher during day hours, thus showing a positive correlation with both signal rms and HVSR peak amplitude. For these sites we analysed also body waves of local earthquakes and T waves produced by regional earthquakes in order to compute the HVSR of signals composed predominantly by body waves. Results of body waves and *T* waves are more similar to the HVSR of day hour seismic noise than the HVSR of night hour seismic noise, thus suggesting that the stronger seismic noise recorded during day hour may contain a greater amount of body waves with respect to the night hour noise.

Key words: Body waves; Seismic noise; Site effects; Wave propagation.

INTRODUCTION

The seismic noise is often a matter of study because it carries useful information about the shallow geological structure and seismic site effects. The nature and composition of the background seismic signal has been investigated by many authors for various purposes in the past decades. It is proven that long period and low frequency noise up to about 1 Hz is composed predominantly by surface waves of natural origin mostly related with weather conditions at local and regional distances (Bonnefoy-Claudet *et al.* 2006). On the contrary, the wavefield of high frequency ($f > 1$ Hz) seismic noise is much more complex because it contains a lot of signals produced by artificial sources. A significant amount of body waves in the high frequency seismic noise has been established by some studies (Bonnefoy-Claudet *et al.* 2006; Zhang *et al.* 2009; Koper *et al.* 2010; Peruzzetto *et al.* 2018). The important contribution of artificial sources is the origin of the daily and weekly cycles widely observed in the amplitude of high frequency seismic noise. This is particularly evident in urban environment and surrounding areas (Cara *et al.* 2003, 2010; Guillier *et al.* 2007; La Rocca & Galluzzo 2012).

The horizontal to vertical spectral ratio (HVSR) of seismic noise has become a common tool in the investigation of site effects (Nakamura 1989; Lermo & Chavez-Garcia 1994; Mucciarelli 1998; Mucciarelli & Gallipoli 2001; Parolai *et al.* 2010; Chavez-Garcia *et al.* 2018; Napolitano *et al.* 2018; Perron *et al.* 2018; and many others). After the paper by Nakamura (1989), this method has been applied by hundreds of researchers in various environments. The aim of most applications is to characterize the soil response to a seismic input. The HVSR method has proven very efficient in the estimation of the resonance frequency of a soft layer upon bedrock (Bard *et al.* 2004). In such a case the method is also well supported by theoretical basis. The peak in the HVSR is explained by the resonance of *S* waves (Nakamura 1989, 2000) and/or by the ellipticity of Rayleigh waves that change with frequency becoming a horizontal linear motion when the vertical component vanishes at the resonance frequency of the surface layer (e.g. Fah *et al.* 2001; Bard *et al.* 2004; Lontsi *et al.* 2019). On the contrary, when the shallow geological structure is complex an exhaustive comprehension of the relationship between soil structure and HVSR is still missing. The interpretation of HVSR and its relation with site effects may be further complicated by local topography, which can amplify the ground motion in some frequency band (Chavez-Garcia *et al.* 1996, 1997; Paolucci 2002; Massa *et al.* 2010; Panzera *et al.* 2011; Burjanek *et al.* 2014) with important effects on the signal polarization and HVSR (Spudich *et al.* 1996; Formisano *et al.* 2012; Napolitano *et al.* 2018). One criterion that many authors require for a reliable application of the method is the stationarity of seismic noise, although some studies suggest that the presence of transients in the

analysed signal does not compromise the result (Mucciarelli *et al.* 2003; Parolai & Galiana-Merino 2006). The HVSR of seismic noise is widely used nowadays in the characterization of site effects, often in urban areas (Strollo *et al.* 2012; Martorana *et al.* 2018). The noise HVSR curve has been usually assumed to be a stable feature of a given site (Parolai *et al.* 2004), but recently some works have shown results in contrast with such an assumption (Benkaci *et al.* 2018; La Rocca *et al.* 2020; Rigo *et al.* 2021). Here, we describe the variation of HVSR with the day–night cycle of seismic noise observed at some sites. A day–night cycle that occurs at frequency higher than about 1 Hz is a typical feature of seismic noise observed almost everywhere, and particularly in and around urban environment. It is due to the higher contribution of artificial sources active during day hours compared with night hours. Some studies reveal also a weekly cycle tightly related with human activities (Bonnefoy-Claudet *et al.* 2006; Guillier *et al.* 2007; Cara *et al.* 2010; La Rocca & Galluzzo 2012). One debated feature of seismic noise is the relative contribution of body and surface waves in general, and with regard to the artificial sources in particular. The composition of seismic noise, that is the relative amount of body and surface waves versus frequency, and how it changes between day and night, is a matter of study. Defining the composition of a seismic wavefield in a given area could be possible only if an array of three-component seismic stations was available and the investigated area was flat and geologically homogeneous. In that case the analysis of recorded signals with array methods and the polarization analysis would give a detailed characterization of the wavefield composition, allowing for a reliable discrimination between body and surface waves in a frequency range that depends on the array extension and configuration (e.g. Rost & Thomas 2002; Imtiaz *et al.* 2018). Unfortunately, such detailed analysis is seldom possible. In most of the cases, the seismic noise to be analysed is recorded by only one three-component seismic station, and usually for a short time duration.

In this study, we investigate the composition of seismic noise through the comparison of HVSR analysis carried out on seismic noise and earthquakes, which is possible because we use data from a permanent seismic network. In addition to local and regional earthquakes, we analysed also *T* waves generated by earthquakes occurred at regional distances. *T* waves propagate as acoustic waves through the ocean, then they are converted to seismic waves at the ocean-shore interface. *T* waves in the crust normally have the most of energy in the 1.5–6 Hz frequency band. The conversion at the water-crust interface is expected to produce mostly *P* and *SV* waves (De Groot-Hedlin & Orcutt 1999; Talandier & Okal 2016). In case surface waves are also generated at the sea bottom, they travel much slower than body waves (considering the high frequency), thus their contribution is expected to be negligible at the beginning of the *T* wave signal (depending on the distance from the coast). For these reasons *T* waves constitute a good opportunity of handling signals composed essentially by body waves in a wide frequency band and lasting for tens of seconds.

ANALYSIS OF SEISMIC NOISE

In this work, we analysed seismic noise recorded at more than 30 sites in Calabria, Italy (Fig. 1). The most of these sites are seismic stations of the Università della Calabria Seismic Network (Rete Sismica Unical, http://doi.org/doi:10.7914/SN/IY, www.sismocal.org), while others are stations of the Italian Seismic Network (www.ingv.it), and some are temporary stations deployed for specific research purposes. Many months of continuous seismic recordings

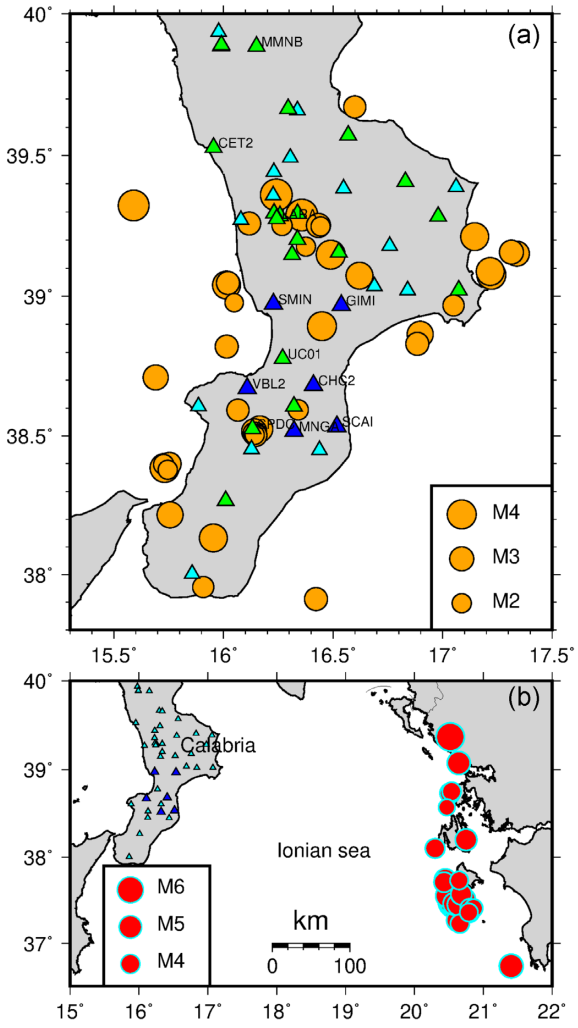

Figure 1. (a) Seismic stations considered in this work (triangle). Different colours represent those sites characterized by one or more well-defined peaks in the HVSR of seismic noise (green), and the sites where a day–night cycle is evident (dark blue). Orange circles show the epicentres of local earthquakes used to compute the HVSR of body waves. (b) Epicentres of regional earthquakes used for the analysis of *T* waves.

were analysed at these sites computing the signal amplitude as the root mean square (rms) averaged among the three components. Fig. 2 shows the signal amplitude in three different frequency bands for one month of data at 7 broad-band seismic stations. The day–night cycle is recognized very well at any sites for frequency higher than 2 Hz, with an important increase of the amplitude during day hours. This is confirmed by a sharp peak at period of 1.0 day in the power spectra (Fig. 2, right plots). In the 0.5–3 Hz frequency band, the day–night cycle is still recognized but the strongest amplitude variations are not periodic. The peak at 1.0 day is still visible in the power spectra, but with a much lower amplitude. At frequency lower than 0.5 Hz the day–night cycle disappears, while the most important amplitude variations, attributed to weather conditions, are characterized by irregular frequency content with the highest amplitude at very long period. We computed also the power spectral density (PSD, mean among the three components) and HVSR on a 600 s window on continuous signals and results were plotted versus time and versus frequency to investigate any variations with time. Fig. 3 shows the results of this analysis at two sites. The results of the same analysis at five more sites are shown in Supporting

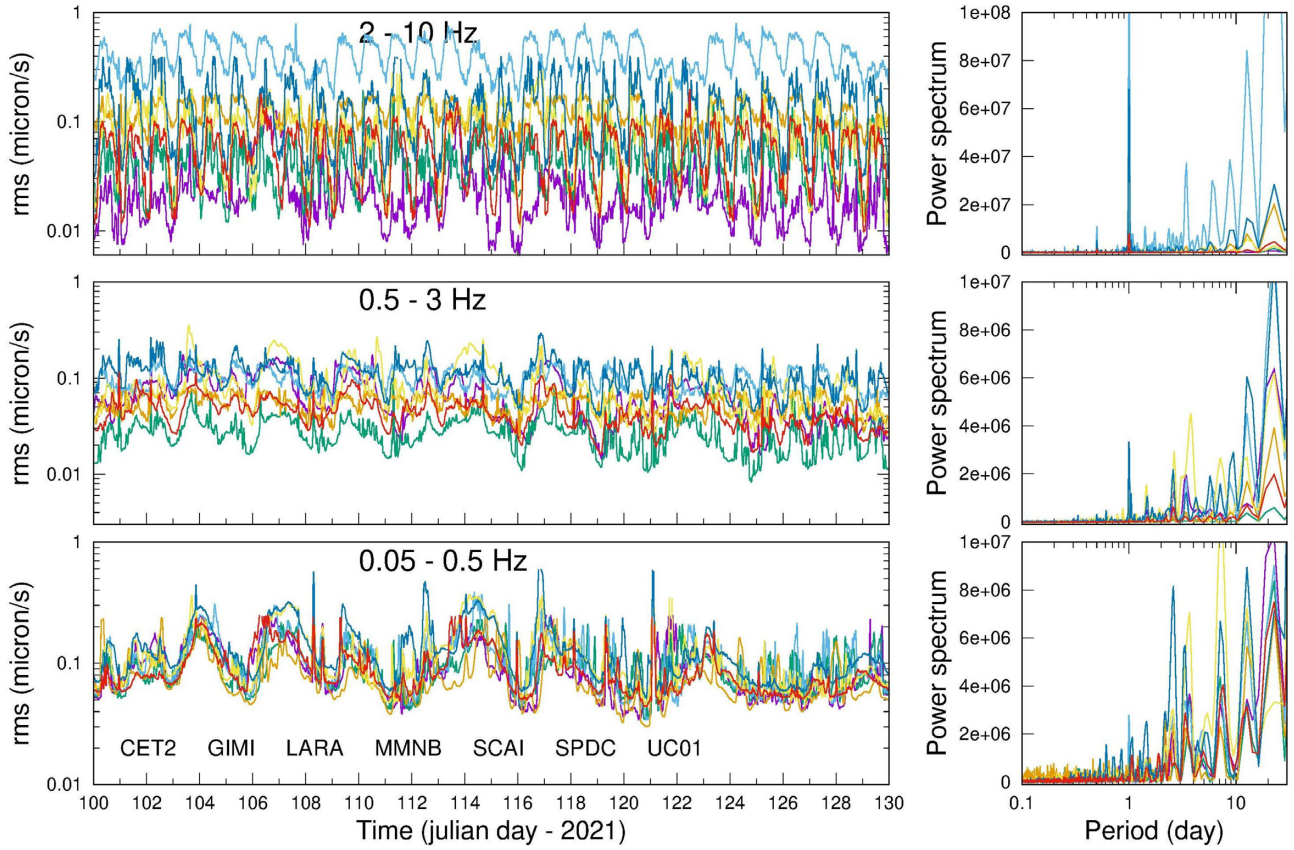

Figure 2. Signal rms amplitude (left plots) at seven sites for 1 month of continuous seismic recordings computed in three frequency bands: 2–10 Hz (a), 0.5–3 Hz (b) and 0.05–0.5 Hz (c), and their corresponding power spectra (right plots). The seismic stations used for this analysis, listed in the bottom left plot, were equipped with broad-band seismometers.

Information Figs S1–S3. Although many of the signals analysed in this work come from broad-band seismic stations, in this paper we focus our attention on the 1–10 Hz frequency band that is the most interesting for the study of site effects related with the shallow geological structure and for seismic risk purposes. For more than 20 of the analysed sites, the HVSR shows at least one peak of amplitude greater than 2 in the frequency range 1–10 Hz, representative of site effects (green and blue symbol in Fig. 1a). In most of the cases, such peaks are likely produced by the local geological structure and/or by the topography of the area. At six of the analysed sites, a clear day–night cycle is also observed in the amplitude of the HVSR peak. Since a day–night cycle is the most typical feature of high-frequency seismic noise, we sought for a correlation between the HVSR peak amplitude and the amplitude of seismic noise. Many of the studied sites are located near some villages, at distances from tens to few hundred metres from houses and roads. The noise PSD variation between day and night is different for each site. During day hours, the seismic noise has a generally higher background amplitude, often with many high-frequency transient signals likely produced by artificial sources nearby. The most common source of such transients is known to be the passage of vehicles nearby. On the contrary, during night hours the amplitude of the background noise is lower in a broad frequency band and the signal looks much more stationary. Therefore, at many studied sites the seismic noise is more stationary during night hours compared with day hours. The HVSR computed for seismic noise recorded at noon and at midnight (local time) is shown in Fig. 4 for the six sites where the difference is more evident.

As a further investigation of the seismic noise composition, we performed a polarization analysis in time domain of continuous seismic recordings. This analysis was applied on 300 s long window of signals bandpass filtered in a narrow frequency band different for each site, centred at the HVSR peak frequency. For each time window we obtain the rectilinearity (RL) of particle motion and the angles of polarization incidence and azimuth, by applying the method of the covariance matrix in time domain (Montalbetti & Kanasevich 1970; Jurkevics 1988; Formisano *et al.* 2012). An example of this analysis applied to 10 days of signals recorded at GIMI site is shown in Fig. 5. For each time window we computed also the rms of the three components ground motion (rms_E, rms_N, rms_Z):

$$\mathrm{rms}_x = \sqrt{\frac{\sum_{j=1}^{N} x_j^2}{N}}$$

and used the three rms_x to compute the average signal rms (mean among the three components rms) and the H/V ratio through the relation:

$$\frac{\mathrm{H}}{\mathrm{V}} = \sqrt{\frac{\mathrm{rms}_E^2 + \mathrm{rms}_N^2}{2\mathrm{rms}_Z^2}}.$$

From this analysis, we obtain rms and H/V ratio versus time, which are representative of the signal bandpass filtered around the frequency of the HVSR peak. Since the H/V ratio is representative of a frequency band, its values are usually smaller than the HVSR peak of the same signals.

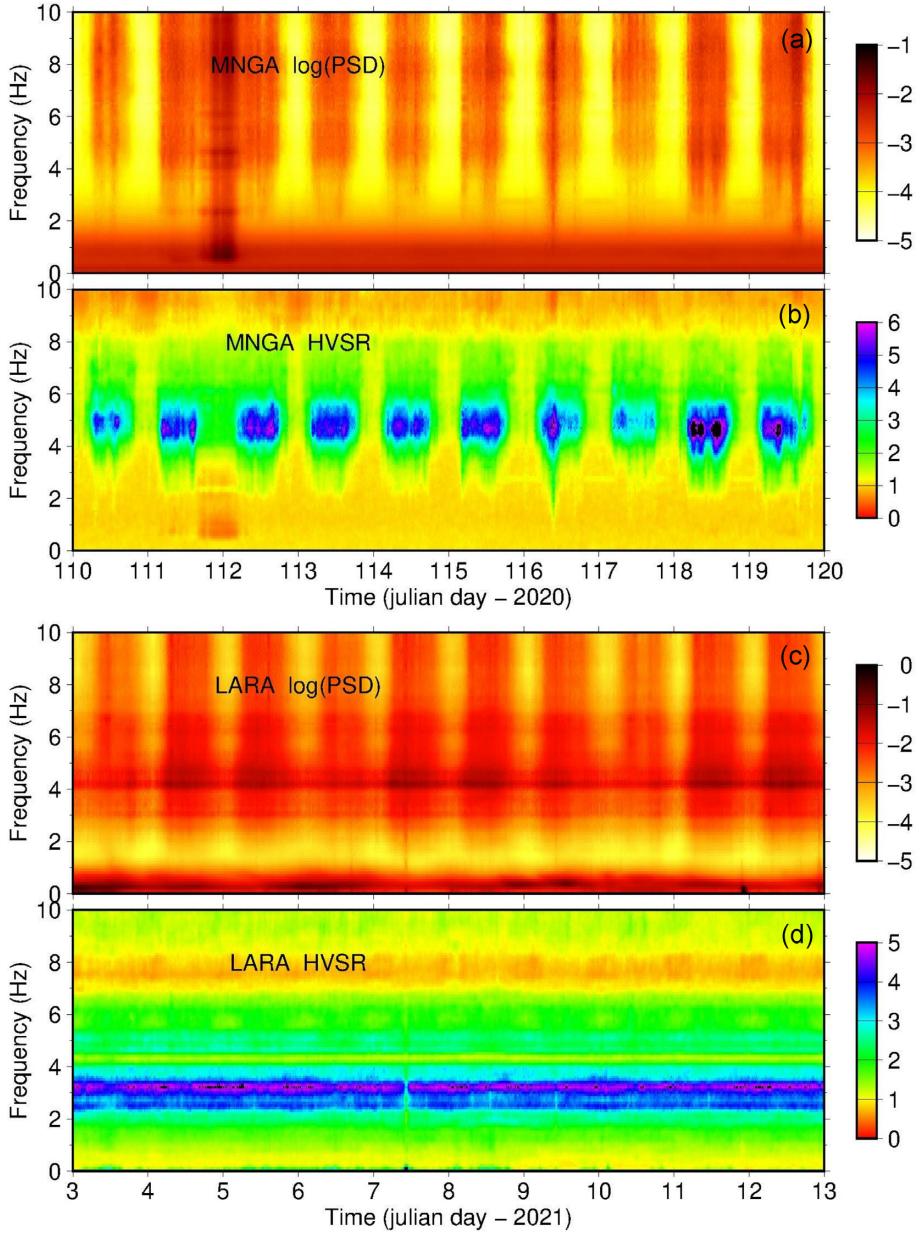

Figure 3. PSD and HVSR versus time and frequency for two sites. Site MNGA is characterized by a strong day–night cycle in both amplitude (a) and HVSR (b). On the contrary, at site LARA a clear day–night cycle is evident in the signal amplitude (c) but no significant variations in time of the HVSR (d).

ANALYSIS OF EARTHQUAKE BODY WAVES AND *T* WAVES

For the sites where a day–night cycle is evident in the HVSR peak amplitude (CHC2, GIMI, MNGA, SCAI, SMIN, VBL2), we calculated the HVSR also for signals in which the contribution of body waves is expected to be largely predominant. The aim of this analysis is an indirect investigation of the difference in the wavefield composition between stationary low level seismic noise recorded by night, and less regular higher amplitude seismic noise recorded during day hours. For this purpose we computed the HVSR for tens of local crustal earthquakes at each studied site. The event selection was different for each site, based on the following requirements: (1) epicentre within 100 km from the recording site; (2) SNR $>$ 5 for a duration of at least 2 min; (3) magnitude greater than 2.8. These criteria ensure that in the analysed signal the seismic noise is negligible and body waves are predominant in the frequency band from 1 to 10 Hz, thus all peaks found in the HVSR of selected sites are included in this analysis. The earthquakes selected for this analysis have magnitude in the range 2.9–4.3, and their epicentres are shown in Fig. 1. The results of HVSR analysis of local earthquakes are shown in Fig. 4 for the six sites characterized by the strongest difference between day and night.

As a further investigation tool, we analysed *T* waves produced by 22 regional earthquakes occurred in the Ionian sea and near the west coast of Greece, with magnitude in the range 4.3–6.8 (Fig. 1). Many earthquakes that occur along the west coast of Greece are very efficient in the generation of *T* waves that propagate westward, and are recorded very well by seismic stations in Calabria. The epicentral distance of the analysed earthquakes ranges from 320 km to more than 500 km (Fig. 1). At such distances *T* waves arrive enough time after the *S* direct wave to have a high signal to coda

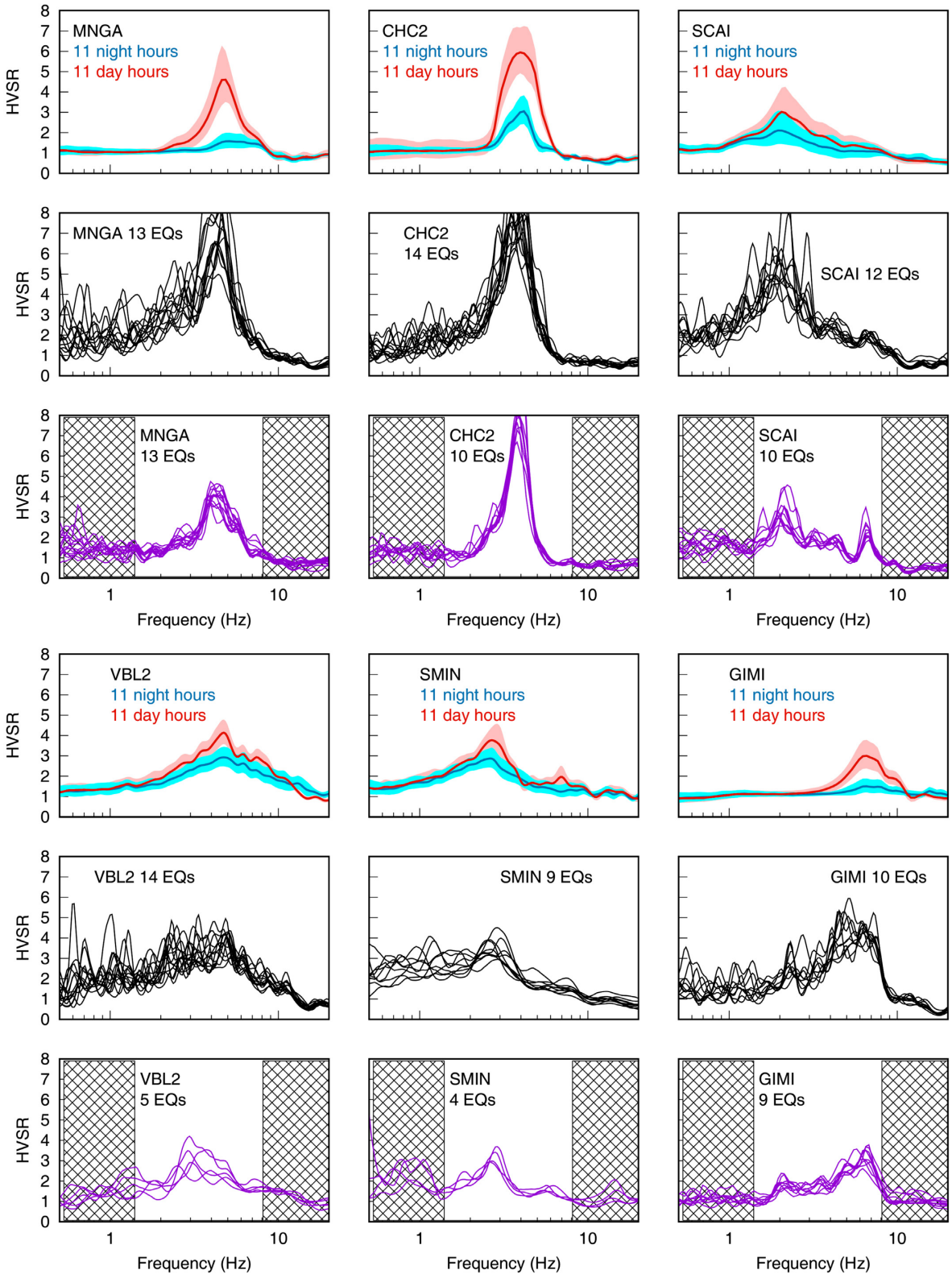

Figure 4. HVSR of seismic noise (plots in rows 1 and 4), earthquakes (plots in rows 2 and 5) and *T* waves (plots in rows 3 and 6) for six sites. Red and blue curves represent the HVSR of day and night hour noise, respectively, with their standard deviation shown by the colour band. The site name is written in each plot, as the number of analysed earthquakes and *T* waves. The results of *T*-wave analysis are fully representative in the 1.5–8 Hz frequency band, while outside of these limits (shadowed areas) the *T* wave to noise ratio may be too small to make reliable the result.

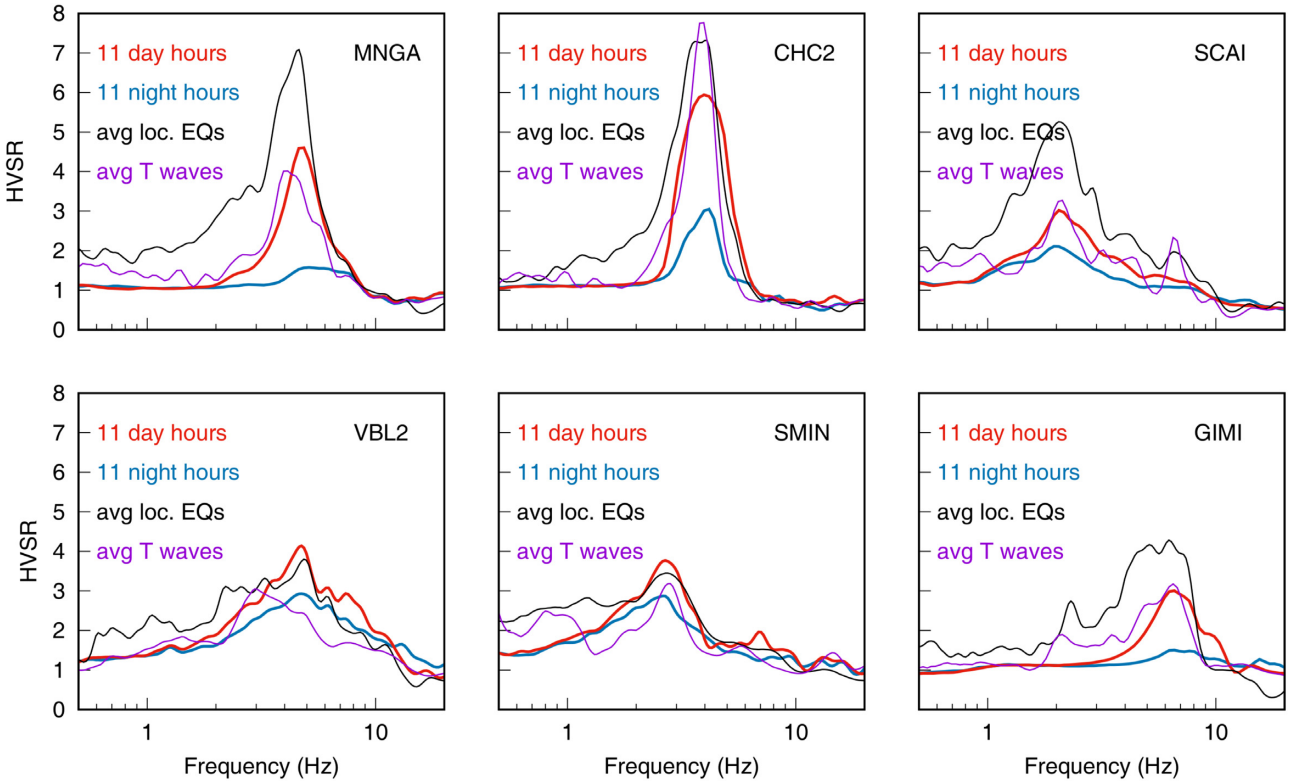

Figure 5. Synthesis of the results of HVSR analysis at the most interesting six sites. Day hour noise (red) and night hour noise (blue) are the same as shown in Fig. 4, while local earthquakes body waves (black) and *T* waves (violet) are the mean among the results shown in Fig. 4 for each site.

waves ratio in the frequency band of our interest (Fig. 7). In many cases they have amplitude even greater than the direct body waves and early *P*- and *S*-coda waves for frequency higher than 1.5 Hz, and they have duration from many tens of seconds to more than a minute. An important feature of T waves is that they are produced as body waves at the land-ocean interface for a time duration much greater than the earthquake source duration. For our purposes, *T* waves are a good opportunity to analyse seismic signals composed predominantly by body waves. *T* waves recorded in Calabria have the most of energy in the 1.5–6 Hz frequency range, but in some cases they have a high SNR up to 10 Hz at the seismic stations very near the coast like SCAI (Fig. 1). The HVSR of *T* waves are shown in Figs 4 and 5 for the six studied sites.

RESULTS

Here, we describe the results of six sites where we observe a significant periodic variation of the HVSR peak amplitude between day and night hours. The correlation between HVSR peak amplitude and signal amplitude is positive, that means the amplitude of HVSR peak is higher during day hours, when the noise amplitude is higher also. Fig. 4 shows the day and night HVSR computed at these stations taking the average value over 11 days considering noise recorded from 11:00 am to 12:00 am, local time, and noise recorded from 1:00 am to 2:00 am, local time. The same figure shows also the HVSR computed for local earthquakes (second row plots) and for *T* waves (third row plots) at the same six sites. For a better comparison among the results of different signals, Fig. 5 shows for each site the average value of the four HVSR types shown in Fig. 4. The frequency of the HVSR peaks is different for each sites (in the range from 2 to 7 Hz), but it is stable in time, taking the same value, or at most values in a narrow frequency range, any time during the day. On the contrary the peak amplitude shows variations between day and night up to a factor 3. At each site the HVSRs of body wave signals are characterized by a common trend (Fig. 4), with the highest peak at frequency equal or very similar to the frequency of the noise HVSR peak. *T* waves show results very similar among them at each site, again with the highest peak at frequency equal or very near to that found from noise and from earthquakes. The HVSRs of earthquakes shown in Fig. 4 are not equal among them because beside site effects they depend also on source effects (through the radiation pattern) and path effects, which are different for each earthquake. On the contrary the results of *T* waves are much more uniform among them at each site because the analysed signals are more self-similar than local earthquake signals. In fact in the *T* wave signals the contributions of source and path are expected to be negligible due to their generation and propagation mechanisms, and the epicentres are located all to the east in a small backazimuth range. Fig. 5 shows for each analysed site the mean values of HVSR computed for day hour noise, night hour noise, local earthquake body waves, and *T* waves, in order to allow for a better comparison of these results among them.

The most impressive results come from sites MNGA and CHC2 (Figs 3–5). At MNGA a very well defined peak at frequency of 4.8 Hz that reaches amplitude almost 5 dominates the HVSR curve during day hours. The same peak practically disappears during night hours. The seismic station is installed at the margin of a very small village, and the surrounding area is characterized by a gentle slope so that topographic effects are expected to be negligible at the peak frequency. The HVSRs of earthquakes are less smooth than that of day hour seismic noise, but they all have the highest peak a frequency very near 4.8 Hz, with amplitude that in some cases is

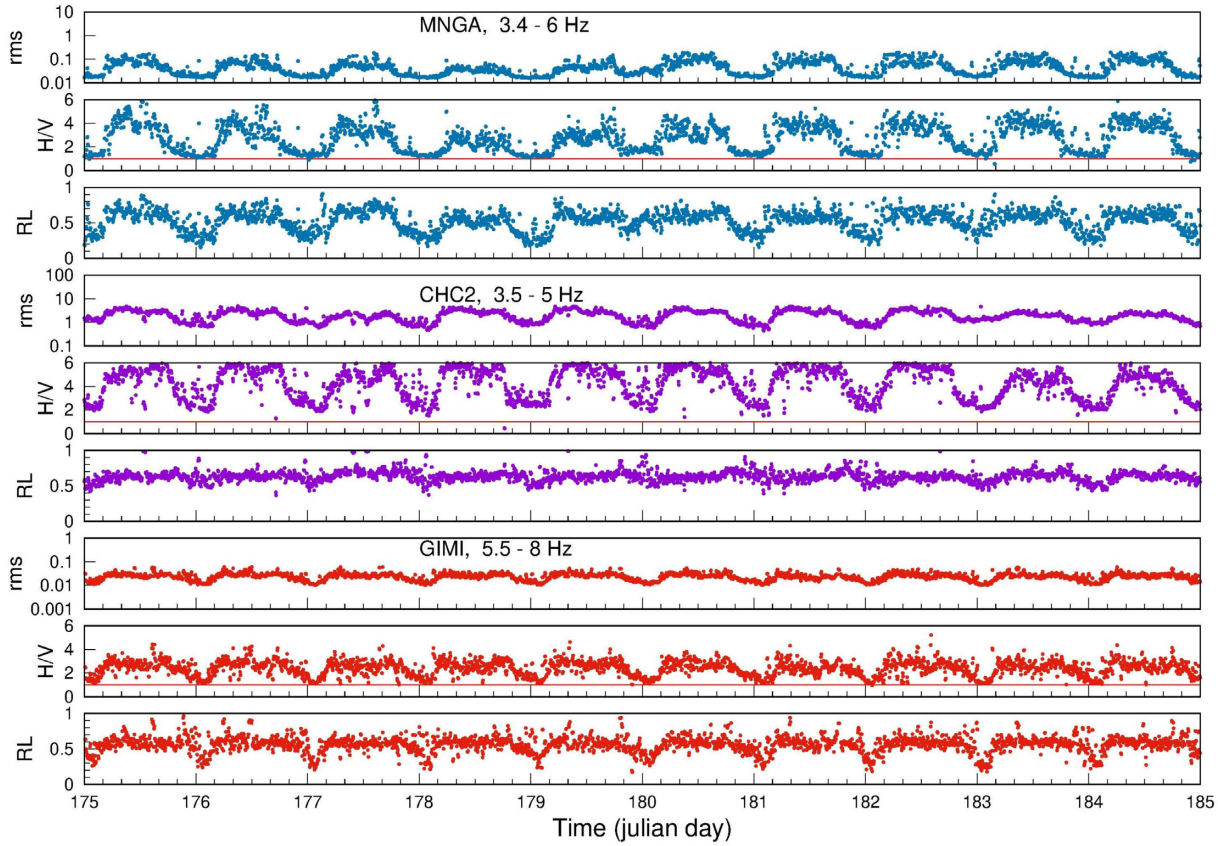

Figure 6. Results of amplitude (rms), H/V and polarization analysis (rectilinearity) for 10 days of continuous seismic recordings at the site MNGA (blue plots), CHC2 (violet plots) and GIMI (red plots). Signals were bandpass filtered as indicated in order to focus the analysis on the high amplitude HVSR peak that characterize each site.

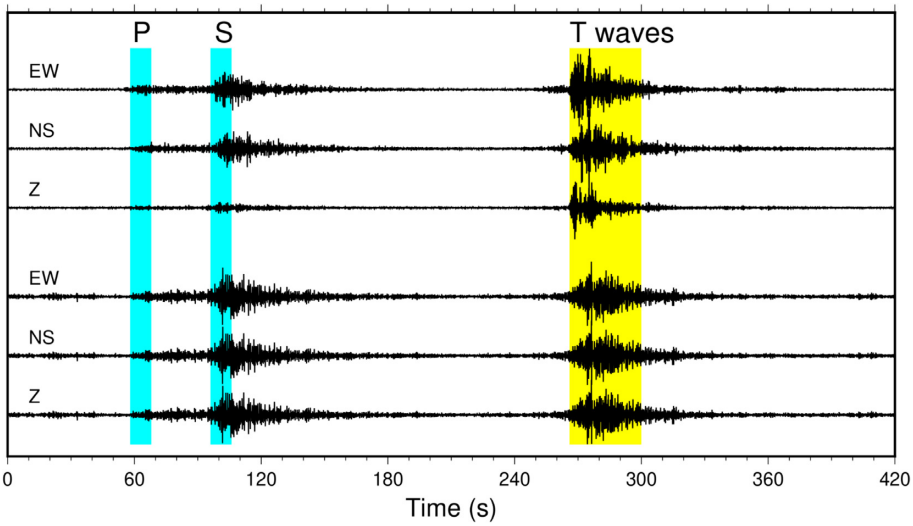

Figure 7. Example of regional earthquakes (20181026235137 and 20181226073754) recorded at site MNGA, characterized by strong *T* waves after the late coda. Seismograms have been bandpass filtered between 1.5 and 6 Hz.

greater than 8. The mean among 14 events is characterized by a peak of amplitude 7 (Fig. 5). The HVSRs of T waves are very uniform among them, with a peak very similar in shape and amplitude to the peak of day hour seismic noise but with frequency a little lower (Figs 4 and 5). At CHC2 the HVSR of seismic noise has always a well defined peak at 4.0 Hz (Figs 4 and 5), but its amplitude changes from about 3 during night hours to 6 or more during day hours. All HVSRs of earthquakes have a high peak at the same frequency, and HVSRs of T waves are the most amazing result of this work: very uniform among them with an impressive peak of amplitude

between 6 and more than 8 at frequency of 4.0 Hz (Figs 4 and 5). The seismic station is installed in a small village on a gentle hillslope and topography effect may give a contribution to the HVSR peak. The site GIMI also shows a consistent difference between day (peak amplitude about 3 at about 7 Hz) and night hours (no peaks at all). Also at this site the HVSR of earthquakes and *T* waves are much more similar to the day hours HVSR than that of night hours. An interesting feature at this site is the small peak at about 2.1 Hz seen in the earthquakes and T waves results, that has no correspondence in the HVSR of seismic noise. Something similar is seen also at SCAI, where a small peak at about 7 Hz in the earthquakes and *T* wave HVSR has no correspondence in the noise results. We do not have an explanation of this result which is likely an effect of the propagation of body waves throughout a complex geological structure. Among the sites that show an evident day–night cycle in the HVSR amplitude we report here SCAI, SMIN and VBL2. At these sites the peak amplitude variation is evident but not so large as seen at the three sites previously described. At VBL2 and SMIN we found only a few regional earthquakes with *T* waves appropriate for our analysis, due to the larger distance from the east coast of these two sites. Looking at Fig. 5 we see that the HVSR of earthquake body waves is the highest at three sites (MNGA, SCAI, GIMI), it is higher than the day hour noise HVSR at four sites (MNGA, CHC2, SCAI, GIMI) and it is always higher than the night hour noise result. Similar considerations hold for T waves HVSR at four sites (MNGA, CHC2, SCAI, GIMI), while at VBL2 and SMIN the difference among the results is not as strong as at the other sites.

Results of the joint rms and polarization analysis, performed on a frequency band centred at the HVSR peak frequency, show very well the day–night cycle in amplitude, H/V and rectilinearity. The RL variation is particularly evident at sites MNGA, CHC2 and GIMI, with a strong positive correlation with the rms and H/V variation, as shown in Fig. 6. During day hours, rms, H/V and RL all take values higher than night hours. The rectilinearity of particle motion is an important parameter to investigate the wavefield composition. An increase of RL during day hours may indicate a lower contribution of Rayleigh waves in the analysed signal compared with night hours, or may correspond to the vanishing of the Rayleigh wave vertical motion which is expected to occur at the resonance frequency.

DISCUSSION AND CONCLUSIONS

The variation in time of the peak amplitude of seismic noise HVSR has been reported in some studies (e.g. Guillier *et al.* 2007; Cara *et al.* 2010; Rigo *et al.* 2021). The analysis of a variety of seismic signals carried out in this work allows to add some important information about the features of seismic noise and its HVSR results. The six sites where we observe a clear day—night cycle in the HVSR peak height are different among them with regard to the shallow geology and topography. Two of them are sites in urban environment (CHC2 and VBL2) with not negligible topographic features. Three sites are in the suburbs of very small villages (GIMI, MNGA, SCAI) while the last site (SMIN) is in mountain environment, some hundreds meters from a very small village. Topography effects are expected to be important for sites SMIN and VBL2, while they must be less important for sites MNGA, CHC2, GIMI and SCAI. Unfortunately a detailed knowledge of the shallow velocity model is not available for the investigated sites, however considering the outcropping geology, ground resonance is expected to be less important at sites SCAI and VBL2 among the six sites.

The comparison of HVSR computed for day and night seismic noise, for local earthquakes and for *T* waves at the six sites described in this work, shows some remarkable feature. At sites where the HVSR peak is stable and persistent but with variable amplitude (CHC2, SCAI, SMIN, Figs 4 and 5), the results are characterized by the same or very similar peak frequency for the four signal types. At the two sites where the peak of night noise is not significant (MNGA and GIMI, Figs 4 and 5), the frequency of the peak obtained from the analysis of day noise and body waves is the same. In any cases the HVSR of earthquake body waves and *T* waves have peak amplitude comparable or greater than the day hour noise, and always greater than the night hour noise. This result suggests that day hour noise has a greater amount of body waves compared with night hour noise. This hypothesis is also partly supported by the results of polarization analysis which shows variations of RL correlated with the increase of signal amplitude during day hours. At sites where local effects are negligible a higher RL would correspond to a lower amount of Rayleigh waves in the analysed signal. On the other hand, at sites where a seismic resonance occur the polarization analysis is not sufficient to measure the amount of Rayleigh waves because at the resonance frequency Rayleigh wave particle motion becomes linearly polarized in the radial direction. From single station data it is not possible to establish the composition of noise signals, therefore we cannot establish if the higher value of RL during day hours corresponds to a greater amount of body waves, or of Love waves, or both. On the other hand Love waves are expected not to be important in the 1–10 Hz frequency range for local small earthquakes, and they must be negligible, if any, in the *T* wave signals. Taking into account all these observations, we argue that the amount of body waves in the analysed frequency range 1–10 Hz in the day hour noise is likely higher than it is during night hour noise. Since the day–night cycle in the HVSR peak amplitude is observed only at some sites, we also conclude that the increase of HVSR peak amplitude during day hours must be a consequence of the interaction of body waves with the local geological structure and topography. The implication of our findings is that much care is needed in the interpretation of HVSR analysis carried out on a short noise recording in all cases where the shallow geology is more complex than a simple horizontally layered structure and topography effects may have a role in the local response. In such cases the results may be quite dependent on the day hour.

For completeness, we have to report that a few of the sites studied in this work are characterized by quite complex variations of noise amplitude and HVSR features, which do not follow a day–night cycle. Some of those sites were studied and described by La Rocca *et al.* (2020), showing a strong relationship between HVSR features and signal amplitude but without a correlation with the day–night cycle. The strange behaviour of some sites regarding their HVSR variations is still beyond our full comprehension.

ACKNOWLEDGMENTS

The authors are grateful to the associate editor and to two anonymous reviewers for their very detailed revision of the original manuscript.

DATA AVAILABILITY

Data used in this work are available on request to the authors.

REFERENCES

Bard, P.Y., SESAME working group, 2004. Guidelines for the implementation of the H/V spectral ratio technique on ambient vibrations measurements, processing and interpretation. SESAME European research project WP12 – Deliverable D23.12.

Benkaci, N., Oubaiche, E.H., Chatelain, J., Bensalem, R., Benouar, D. & Abbes, K., 2018. Non-stability and non-reproducibility of ambient vibration HVSR peaks in Algiers (Algeria), *J. Earthq. Eng.,* **25,** 853–871, doi:10.1080/13632469.2018.1537903.

Bonnefoy-Claudet, S., Cotton, F. & Bard, P.Y., 2006. The nature of noise wavefield and its applications for site effects studies. A literature review, *Earth Sci. Rev.,* **79**(3-4), 205–227.

Burjanek, J., Edwards, B. & Fah, D., 2014. Empirical evidence of local seismic effects at sites with pronounced topography: a systematic approach, *Geophys. J. Int.,* **197,** 608–619.

Cara, F., Di Giulio, G. & Rovelli, A., 2003. A study on seismic noise variations at Colfiorito, central Italy: implications for the use of H/V spectral ratios, *Geophys. Res. Lett.,* **30**(18), 1972.

Cara, F., Di Giulio, G., Milana, G., Bordoni, P., Haines, J. & Rovelli, A., 2010. On the stability and reproducibility of the horizontal-to-vertical spectral ratios on ambient noise: case study of Cavola, Northern Italy, *Bull. seism. Soc. Am.,* **100**(3), 1263–1275.

Chavez-Garcia, F.J., Sanchez, L.R. & Hatzfeld, D., 1996. Topographic site effects and HVSR. A comparison between observations and theory, *Bull. seism. Soc. Am.,* **86**(5), 1559–1573.

Chavez-Garcia, F. J., Rodriguez, M., Field, E.H. & Hatzfeld, D., 1997. Topographic site effects. A comparison of two nonreference methods, *Bull. seism. Soc. Am.,* **87**(6), 1667–1673.

Chavez-Garcia, F.J., Monsalve, H., Gomez-Cano, M. & Vila Ortega, J.J., 2018. Vulnerability and Site effects in earthquake disasters in Armenia (Colombia). I—site effects, *Geosciences,* **8,** 254.

De Groot-Hedlin, C.D. & Orcutt, J.A., 1999. Synthesis of earthquake-generated T waves. *Geophys. Res. Lett.,* **26**(9), 1227–1230.

Fah, D., Kind, F. & Giardini, D., 2001. A theoretical investigati on of average H/V ratios, *Geophys. J. Int.,* **145,** 535–549.

Formisano, L.A., La Rocca, M., Del Pezzo, E., Galluzzo, D., Fischione, C. & Scarpa, R., 2012. Topography effects in the polarization of earthquake signals: a comparison between surface and deep recordings, *Boll. Geofis. Teor. Appl.,* **53**(4), 471–484.

Guillier, B., Chatelain, J.L., Bonnefoy-Claudet, S. & Haghshenas, E., 2007. Use of ambient noise: from spectral amplitude variability to H/V stability, *J. Earthq. Eng.,* **11**(6), 925–942.

Imtiaz, A., Perron, V., Hollender, F., Bard, P.Y., Cornou, C., Svay, A. & Theodoulidis, N., 2018. Wavefield characteristics and spatial incoherency: a comparative study from Argostoli rock- and soil-site dense seismic arrays, *Bull. seism. Soc. Am.,* **108,** 2839–2853.

Jurkevics, A., 1988. Polarization analysis of three-component array data. *Bull. seism. Soc. Am.,* **78,** 1725–1743.

Koper, K.D., Seats, K. & Benz, H., 2010. On the composition of Earth's short-period seismic noise field, *Bull. seism. Soc. Am.,* **100**(2), 606–617.

La Rocca, M. & Galluzzo, D., 2012. A seismic array in the town of Pozzuoli in Campi Flegrei (Italy), *Seismol. Res. Lett.,* **83**(1), 86–96.

La Rocca, M., Chiappetta, G.D., Gervasi, A. & Festa, R.L., 2020. Non-stability of the noise HVSR at sites near or on topographic heights, *Geophys. J. Int.,* **222,** 2162–2171.

Lermo, J. & Chavez-Garcia, J., 1994. Are microtremors useful in site response evaluation?, *Bull. seism. Soc. Am.,* **84**(5), 1350–1364.

Lontsi, A.M. *et al.*, 2019. A generalized theory for full microtremor horizontal-to-vertical [H/V(z, f)] spectral ratio interpretation in offshore and onshore environments, *Geophys. J. Int.,* **218,** 1276–1297.

Martorana, R., Capizzi, P., D'Alessandro, A., Luzio, D., Di Stefano, P., Renda, P. & Zarcone, G., 2018. Contribution of HVSR measures for seismic microzonation studies, *Ann. Geophys.,* **61**(2), SE225.

Massa, M., Lovati, S., D'Alema, E., Ferretti, G. & Bakavoli, M., 2010. An experimental approach for estimating seismic amplification effects at the top of a ridge, and the implication for ground-motion predictions: the case of Narni, Central Italy, *Bull. seism. Soc. Am.,* **100**(6), 3020–3034.

Montalbetti, J.F. & Kanasewich, E.R., 1970. Enhancement of teleseismic body phases with a polarization filter, *Geophys. J. R. astr. Soc.,* **21,** 119–129.

Mucciarelli, M., 1998. Reliability and applicability of Nakamura's technique using microtremors: an experimental approach, *J. Earthq. Eng.,* **2,** 625–638.

Mucciarelli, M. & Gallipoli, M.R., 2001. A critical review of 10 years of microtremor HVSR technique, *Boll. Geofis. Teor. Appl.,* **42**(3-4), 255–266.

Mucciarelli, M., Gallipoli, M.R. & Arcieri, M., 2003. The stability of the horizontal-to-vertical spectral ratio of triggered noise and earthquake recordings, *Bull. seism. Soc. Am.,* **93**(3), 1407–1412.

Nakamura, Y., 1989. A method for dynamic characteristics estimations of subsurface using microtremors on the ground surface, *Q. Rep. Railw. Tech. Res. Inst. Japan,* **30,** 25–33.

Nakamura, Y., 2000. Clear identification of fundamental idea of Nakamura's technique and its applications, in *Proceedings of XII World Conf. Earthquake Engineering,* New Zealand, Paper no 2656.

Napolitano, F., Gervasi, A., La Rocca, M., Guerra, I. & Scarpa, R., 2018. Site effects in the Pollino region from spectral and polarization analyses of seismic noise and earthquakes, *Bull. seism. Soc. Am.,* **108,** 309–321.

Panzera, F., Lombardo, G. & Rigano, R., 2011. Evidence of topographic effects through the analysis of ambient noise measurements, *Seismol. Res. Lett.,* **82,** 413–419.

Paolucci, R., 2002. Amplification of earthquake ground motion by steep topographic irregularities, *Earthq. Eng. Struct. Dyn.,* **31,** 1831–1853.

Parolai, S. & Galiana-Merino, J.J., 2006. Effect of transient seismic noise on estimates of H /V spectral ratios, *Bull. seism. Soc. Am.,* **96**(1), 228–236.

Parolai, S., Richwalski, S.M., Milkereit, C. & Bormann, P., 2004. Assessment of the stability of H/V spectral ratios from ambient noise and comparison with earthquake data in the Cologne area (Germany), *Tectonophysics,* **390**(1), 57–73.

Parolai, S. *et al.*, 2010. Site effects assessment in Bishkek (Kyrgyzstan) using earthquake and noise recording data, *Bull. seism. Soc. Am.,* **100**(6), 3068–3082.

Perron, V., Gélis, C., Froment, B., Hollender, F., Bard, P.-Y., Cultrera, G. & Cushing, E.M., 2018. Can broad-band earthquake site responses be predicted by the ambient noise spectral ratio? Insight from observations at two sedimentary basins, *Geophys. J. Int.,* **215,** 1442–1454.

Peruzzetto, M., Kazantsev, A., Luu, K., Metaxian, J.P., Huguet, F. & Chauris, H., 2018. Broad-band ambient noise characterization by joint use of cross-correlation and MUSIC algorithm, *Geophys. J. Int.,* **215,** 760–779.

Rigo, A., Sokos, E., Lefils, V. & Briole, P., 2021. Seasonal variations in amplitudes and resonance frequencies of the HVSR amplification peaks linked to groundwater, *Geophys. J. Int.,* **226,** 1–13.

Rost, S. & Thomas, C. 2002. Array seismology: methods and applications, *Rev. Geophys.,* **40**(3), 1008.

Spudich, P., Hellweg, M. & Lee, W.H.K., 1996. Directional topographic site response at Tarzana observed in aftershocks of the 1994 Northridge, California, earthquake: implications for mainshock motions, *Bull. seism. Soc. Am.,* **86**(1B), S193–S208.

Strollo, A., Parolai, S., Bindi, D., Chiauzzi, L., Pagliuca, R., Mucciarelli, M. & Zschau, J., 2012. Microzonation of Potenza (Southern Italy) in terms of spectral intensity ratio using joint analysis of earthquakes and ambient noise, *Bull. Earthq. Eng.,* **10**(2), 493–516.

Talandier, J. & Okal, E.A., 2016. A new source discriminant based on frequency dispersion for hydroacoustic phases recorded by T-phase stations, *Geophys. J. Int.,* **206,** 1784–1794.

Zhang, J., Gerstoft, P. & Shearer, P.M., 2009. High-frequency P-wave seismic noise driven by ocean winds, *Geophys. Res. Lett.,* **36,** L09302, doi:10.1029/2009GL037761.

SUPPORTING INFORMATION

Supplementary data are available at *GJI* online.

Figure S1. PSD and HVSR versus time and frequency for sites GIMI and CHC2, both characterized by a strong day–night cycle in both amplitude (a and c) and HVSR (b and d).

Figure S2. PSD and HVSR versus time and frequency for sites VBL2 and SMIN, both characterized by a clear day–night cycle in both amplitude (a and c) and HVSR (b and d).

Figure S3. PSD and HVSR versus time and frequency for site SCAI, characterized by a clear day–night cycle in both amplitude (a) and HVSR (b).

Please note: Oxford University Press is not responsible for the content or functionality of any supporting materials supplied by the authors. Any queries (other than missing material) should be directed to the corresponding author for the paper.

Day-night cycle of seismic noise HVSR and comparison with body waves and T waves

Mario La Rocca, Giuseppe Davide Chiappetta

Supplementary material

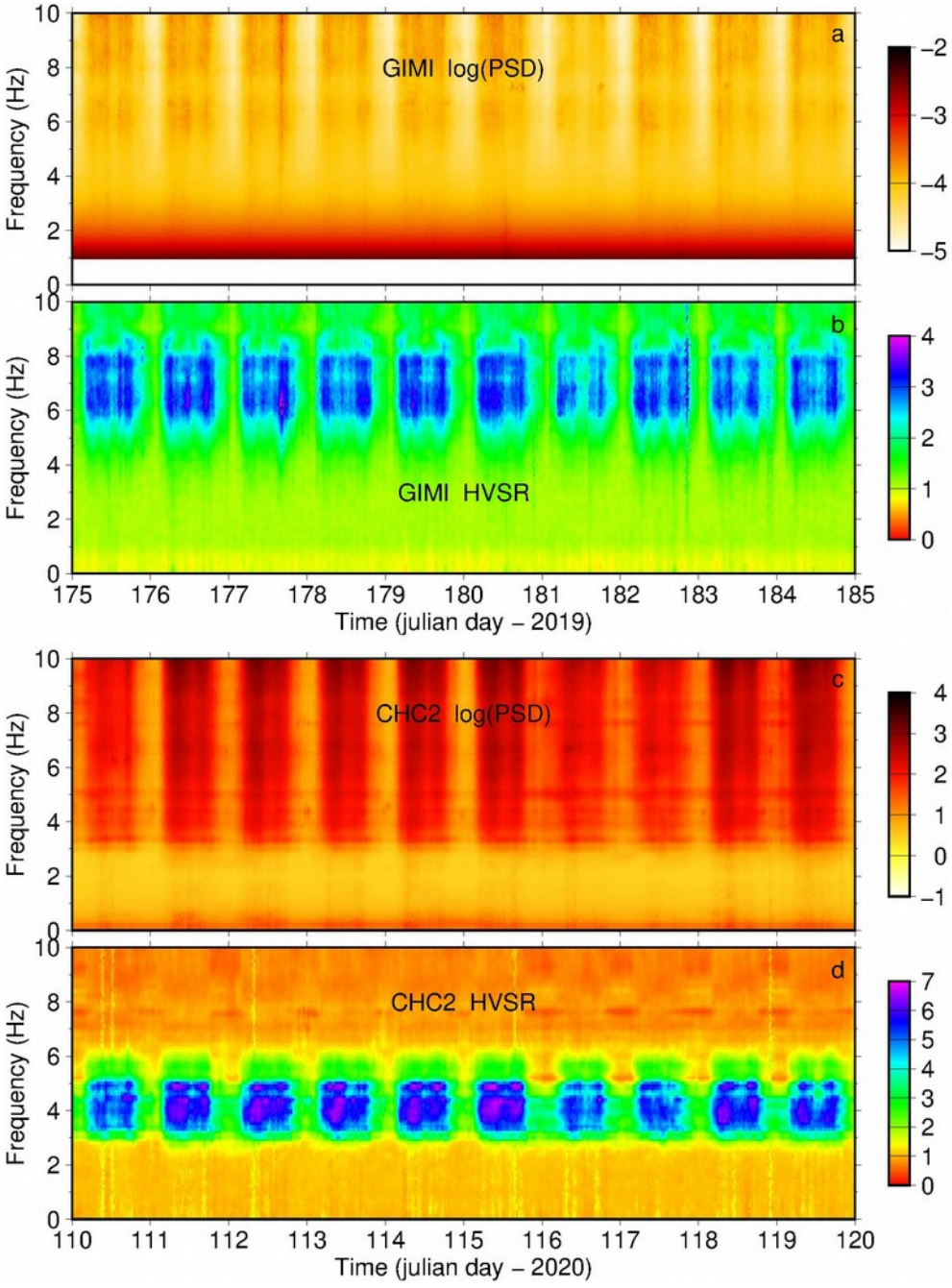

Figure S1. PSD and HVSR versus time and frequency for sites GIMI and CHC2, both characterized by a strong day-night cycle in both amplitude (a, c) and HVSR (b, d).

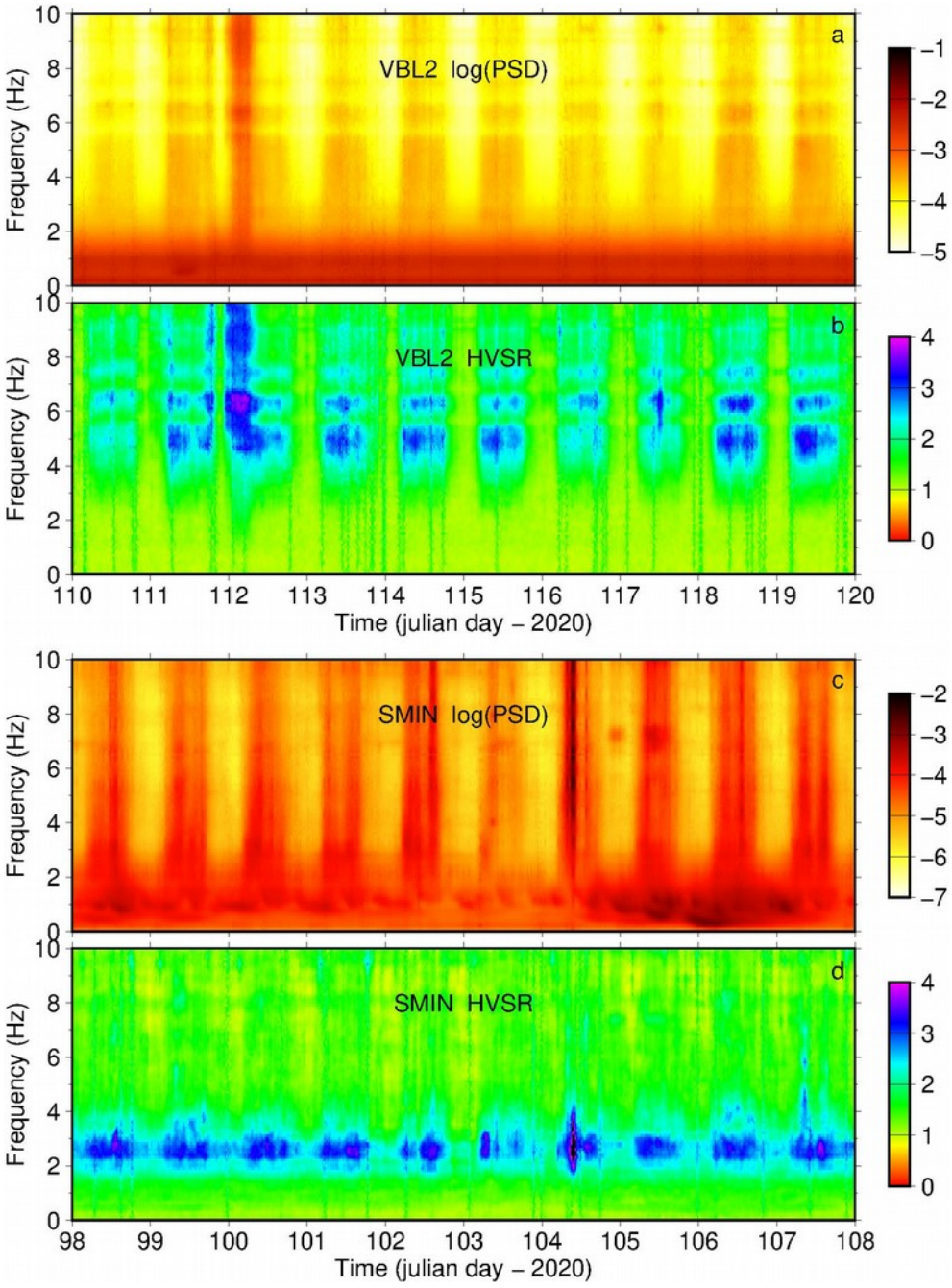

Figure S2. PSD and HVSR versus time and frequency for sites VBL2 and SMIN, both characterized by a clear day-night cycle in both amplitude (a, c) and HVSR (b, d).

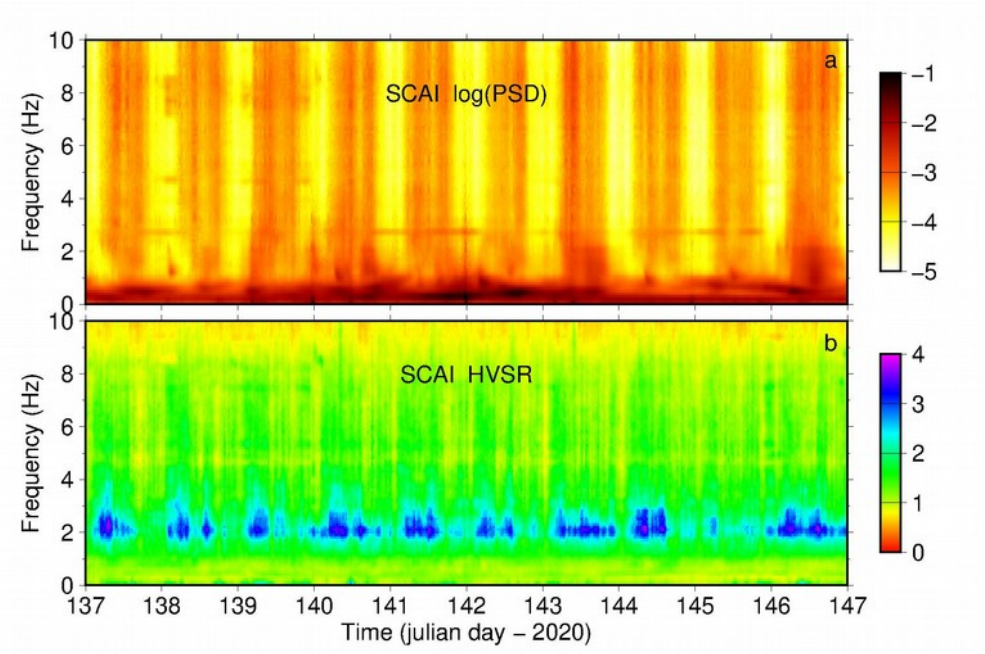

Figure S3. PSD and HVSR versus time and frequency for site SCAI, characterized by a clear day-night cycle in both amplitude (a) and HVSR (b).